

Methodology for the study of modified jet-like topologies in heavy ion collisions via three particle correlation functions

N. N. Ajitanand, J. M. Alexander, Roy A. Lacey, and A. Taranenko
*Department of Chemistry, Stony Brook University,
 Stony Brook, NY, 11794-3400, USA*

(Dated: July 4, 2018)

Methodology is presented for analysis of three-particle correlation functions obtained in heavy ion collisions at ultra-relativistic energies. We show that harmonic correlations can be removed and jet driven correlations reliably extracted. Results from detailed Monte Carlo simulations are used to demonstrate the efficacy of this technique for the study of modifications to away-side jet topologies. Such modifications are an essential probe of the properties of the quark gluon plasma produced in heavy ion collisions.

PACS numbers: PACS 25.75.Ld

I. INTRODUCTION

Studies of ultra-relativistic heavy ion collisions have provided a wealth of evidence for the creation of a new state of matter in a collision zone of very high energy density [1, 2, 3, 4], historically termed the quark gluon plasma QGP. As the properties of this matter are being explored and characterized, it may be that new terminology will be chosen to be more suggestive of its actual properties, as they are revealed. Current research is actively directed toward measurements of these properties.

One of the major tools for such measurements has been the study of correlations between the observed particles which emanate from the collision medium following its expansion and ultimate hadronization. For example, much detailed information has been obtained for the so called “harmonic flow” correlations between individually selected particles and the reaction plane (e.g. the second harmonic coefficient (v_2)) as a function of particle identity PID, collision centrality, transverse momentum p_T , and rapidity η [5, 6, 7, 8, 9, 10, 11, 12, 13, 14]. From the set of systematic data, initial estimates have been made of the speed of sound in the QGP, the ratio of its viscosity to entropy density, its bulk viscosity and other properties [14, 15, 16, 17, 18, 19, 20, 21, 22].

Formation of the collision medium is sometimes accompanied by hard parton-parton scatterings. These scattered partons can interact strongly with the medium and lose energy as they propagate through it, before fragmenting into jets of hadrons [23, 24, 25]. Such energy loss can lead to a strong modification of both the yield and the topological patterns of jets [26, 27]. This gives another detailed experimental probe of the medium which is currently being explored and developed via measurements of di-jet correlations [26, 27, 28, 29, 30, 31].

Techniques for the study of jet-induced two-particle azimuthal angle correlations are well advanced, and results are being accumulated for systematic evaluation. In p+p and d+Au collisions, these jets of hadrons are found essentially back-to-back in azimuth i.e. $\Delta\phi \sim 180^\circ$ [32]. By contrast, the observed di-jet topologies in Au+Au collisions are found to be significantly mod-

ified [26, 27, 28, 29, 30, 31], presumably due to parton medium interactions that occur on passage of the parton through the reaction medium. One very intriguing result of these di-jet studies is the observation of broadening of the away-side jet, and even the displacement of its most probable angle away from $\Delta\phi = 180^\circ$ [26, 27]. Several mechanistic scenarios have been proposed for this observation; they include Čerenkov gluon radiation [33], conical flow [34, 35, 36, 37, 38, 39] and deflected or “bent” jets [40, 41]. To date, the characteristic p_T dependent patterns predicted for Čerenkov gluon radiation [33] have not been observed. The confirmation of a conical flow signal would not only give a direct probe of the equation of state (EOS) of hot QCD matter, but also an important constraint for an upper limit for the viscosity of the medium [34, 35, 38, 39].

Two particle correlation measurements do not provide an unambiguous distinction between conical flow and deflected jets. However, the topological information afforded by the correlations between three or more particles can. Here, we lay out a method of analysis for three particle correlations which demonstrates a topological distinction between conical flow and deflected (or bent) jets. We follow and build on methodology formerly presented for the study of two-particle correlations; namely, the use of normalized correlation functions and extensive testing via Monte Carlo reaction simulations [42]. To focus on the di-jet-like characteristics, we exploit a novel coordinate system that is most intuitive and natural for visualizing di-jet topologies.

II. TWO-PARTICLE CORRELATION FUNCTIONS

In reference [42] we presented a method for constructing and analyzing two particle correlation functions based on the relative laboratory azimuthal angle $\Delta\phi$, for particle pairs. In brief, jet correlations were emphasized by selecting events with at least one high transverse momentum p_T (trigger) particle. Each trigger particle was then paired with associated particles of a lower p_T to obtain

the pair correlation function $C_2(\Delta\phi)$;

$$C_2(\Delta\phi) = \frac{N_R(\Delta\phi)}{N_M(\Delta\phi)}, \quad (1)$$

where $N_S(\Delta\phi)$ and $N_M(\Delta\phi)$ are normalized same-events and mixed-events distributions and $\Delta\phi = |\phi_1 - \phi_2|$ is the difference between the azimuthal angles of the particle pair. The same-events distribution was constructed from particle pairs obtained from the same event; the mixed-events distribution was constructed by selecting each particle in a given pair from a different events having similar centrality and collision vertex positions.

A. Extraction of Jet Shapes

Using a two component model ansatz, we showed [42] that the pair correlation from a combination of flow and jet sources is given by;

$$C_2(\Delta\phi) = b_0[C_H(\Delta\phi) + C_J(\Delta\phi)], \quad (2)$$

where the flow contribution $C_H(\Delta\phi)$ can be estimated as

$$C_H(\Delta\phi) = [1 + 2v_2^2 \cos 2(\Delta\phi) + 2v_4^2 \cos 4(\Delta\phi)], \quad (3)$$

and $C_J(\Delta\phi)$ is the jet function that needs to be evaluated. It is noteworthy that no explicit or implicit assumption is made for the functional form of $C_J(\Delta\phi)$. By rearrangement of Eq. 2 one obtains

$$C_J(\Delta\phi) = \frac{C_2(\Delta\phi) - b_0 C_H(\Delta\phi)}{b_0}. \quad (4)$$

Thus, knowledge of b_0 is required to evaluate the jet-like function $C_J(\Delta\phi)$. It is clear from Eq. 4 that b_0 is influenced by the jet function which is being sought after, and an approximation is required to aid the evaluation of b_0 . After extensive detailed simulation studies, we concluded that a reasonable assumption for the extraction of reliable jet-like functions is the zero yield at minimum (ZYAM) condition – that the di-jet function has a zero yield at minimum [42];

$$b_0 C_H(\Delta\phi_{min}) = C_2(\Delta\phi_{min}), \quad (5)$$

which can be solved to obtain b_0 . This procedure allows reliable extraction of jet-like topologies and a lower limit for jet-like per trigger yields.

B. Simulations

Reaction simulations were used to extensively test this analysis approach. The requisite simulations were carried out on an event-by-event basis with the following essential steps:

- First, the reaction plane orientation was chosen.

- Particles were then emitted with p_T and multiplicity according to the observed distributions.
- For flowing particles, the azimuthal angle for each particle ϕ_i was chosen to give a harmonic distribution with respect to the angle of the reaction plane ψ_R :

$$N(\phi - \psi_R) \propto [1 + 2v_2 \cos 2(\phi - \psi_R) + 2v_4 \cos 4(\phi - \psi_R)] \quad (6)$$

where $v_{2,4}$ are Fourier coefficients which characterize the strength of the flow.

- For jets, the orientation of the lead- or near-side axis was chosen with a random azimuth. For “normal” jets, the away-side axis was oriented opposite to the lead-axis on average.
- The lead-jet particles were emitted clustered about the lead-axis. The away-side jet particles were emitted clustered about the away-side axis.

Simulations were performed both for an ideal detector and for the PHENIX detector. A detailed description of the latter can be found in Ref. [43]. As outlined in Ref. [42], the simulations indicated that, even for cases in which strongly distorted away-side jets were introduced, the decomposition method retrieved the shape of the input jet function in detail, confirming that the decomposition procedure is robust.

We now turn to the discussion of three particle correlation functions.

III. THREE-PARTICLE CORRELATION FUNCTIONS

Analogous to $C_2(\Delta\phi)$, three particle correlation functions can be constructed from particle triplets comprised of one high p_T trigger particle (i) and two associated particles of lower p_T (j and k). To focus on three-particle jet-like correlations, we transform the lab angles $(\theta_{lab}, \phi_{lab})$ of each particle to (θ^*, ϕ^*) in a new frame whose z axis is the direction of the high p_T trigger hadron. This coordinate frame is illustrated in Fig. 1(a). In this frame, the three particle correlation function is given by the ratio of two distributions:

$$C_3(\theta^*, \Delta\phi^*) = \frac{N_S(\theta^*, \Delta\phi^*)}{N_M(\theta^*, \Delta\phi^*)}, \quad (7)$$

where $N_S(\theta^*, \Delta\phi^*)$ and $N_M(\theta^*, \Delta\phi^*)$ are normalized 2D-distributions for the same- and mixed-events respectively. Here, θ^* is the polar angle of one of the two associated hadrons and $\Delta\phi^* = |\phi_j^* - \phi_k^*|$ is the difference between their azimuthal angles. The same-events distribution was obtained via event-by-event selection of particle triplets from the same event. For mixed-events, particle triplets were obtained by selecting each member from a different event.

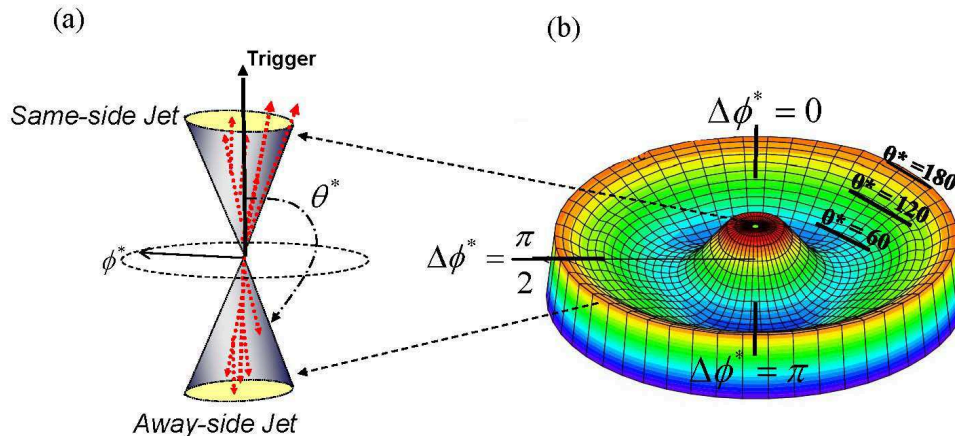


FIG. 1: (a) Schematic illustration of the coordinate system used for the construction of three-particle correlation functions comprised of high p_T trigger particle and two low p_T associated particles. The lab angles $(\theta_{lab}, \phi_{lab})$ of each particle is transformed to (θ^*, ϕ^*) in a new frame whose z axis is the direction of the high p_T trigger. (b) Polar plot of a simulated three-particle correlation function for a normal di-jet. The polar angle θ^* , of one of the associated low p_T particles in the new frame, is plotted along the radial axis; the difference between the azimuthal angles $\Delta\phi^*$, of the two associated hadrons in the new frame (see text) is plotted along the azimuthal axis.

The correlation function so obtained is best viewed in the polar representation shown in Fig. 1(b), where a simulated three particle correlation surface is shown. Both flow and di-jet correlations were incorporate in the simulation. In Fig. 1(b), θ^* and $\Delta\phi^*$ indicate the radial and azimuthal axes respectively. In this polar representation, the near-side jet is indicated by a peak at the center of the plot ($\theta^* = 0^0$) and the characteristic ridge at $\theta^* = 180^0$ signals a normal or unmodified away-side jet (i.e. a back-to-back jet).

The primary objective of our study is to use such correlation surfaces to distinguish between different mechanistic scenarios for away-side jet modification which can not be discerned via two-particle correlation functions. To demonstrate this ability we used our simulation code to model di-jets with (i) an away-side bent jet and (ii) an away-side “cone” jet (see illustrations in Figs. 2(a) and (c) respectively). For the first, the away-side jet axis is bent to an angle of $\sim 120^0$ with respect to the lead-jet axis and the away-side jet particles are emitted clustered about this axis. The axis for the away-side cone jet was chosen opposite (on average) to the lead-axis, and its associated jet-like particles were emitted so as to mimic a Mach cone with Mach angle $\theta_M \sim 60^0$. It is important to note here that these simulations were performed for the PHENIX detector acceptance. Equally important is the fact that model parameters for the simulations were tuned (with insight from experimental data) to give the same shape for the simulated jet-pair correlation functions for bent- and cone jets, as shown in Fig. 2(b). For this simulation set, an isotropic underlying event was employed.

Figure 2(a) gives an illustration of a di-jet with a bent away-side jet. The corresponding simulated three par-

ticle correlation function is shown in Fig. 2(d). This correlation surface exhibits a sizable peak at $\theta^* = 0^0$ corresponding to the lead- or same-side jet, and a ridge at $\theta^* = 120^0$ corresponding to the away-side jet, shifted, on average, by $\sim 60^0$ from $\theta^* = 180^0$. The projection of $\Delta\phi^*$ for $\theta^* \sim 120^0$ (i.e around the ridge) is shown in Fig. 2(e); it shows a relatively large peak near $\Delta\phi^* = 0^0$, which results from particle triplets comprised of a high p_T trigger from the near-side jet and two low p_T associated particles from the away-side jet. Two small peaks can also be observed at $\Delta\phi^* \sim 90^0$ and 270^0 in Fig. 2(d); they result from particle triplets in which the high p_T trigger and one low p_T particle is from the same-side jet, but the second low p_T particle is from the away-side jet. The fall-off at large $\Delta\phi^*$ angles reflects the influence of the PHENIX detector acceptance as discussed below.

Figure 2(f) shows the three particle correlation surface for a di-jet with an away-side Mach cone (see illustration in Fig. 2(c)). Analogous to Fig. 2(d), a near-side peak at $\theta^* = 0^0$, and an away-side ridge near $\theta^* = 120^0$ is apparent. However, in contrast to the case for the bent jet, the peak at or near $\Delta\phi^* = 0^0$ is less pronounced. This distinctive signal is made more transparent in Fig. 2(e) where the azimuthal projections ($\Delta\phi^*$ along the ridge) for the away-side bent jet and Mach cone are compared. These correlations result from particle triplets comprised of a high p_T trigger from the same-side jet and two low p_T particles from the away-side Mach cone. As in the case of the bent jet, the two small peaks at $\Delta\phi^* \sim 90^0$ and 270^0 in Fig. 2(f), reflects “anomalous” particle triplets in which the high p_T trigger and one low p_T particle is from the same-side jet and the second low p_T particle is from the away-side Mach cone.

Intuitively, correlated triplets which result from a near-

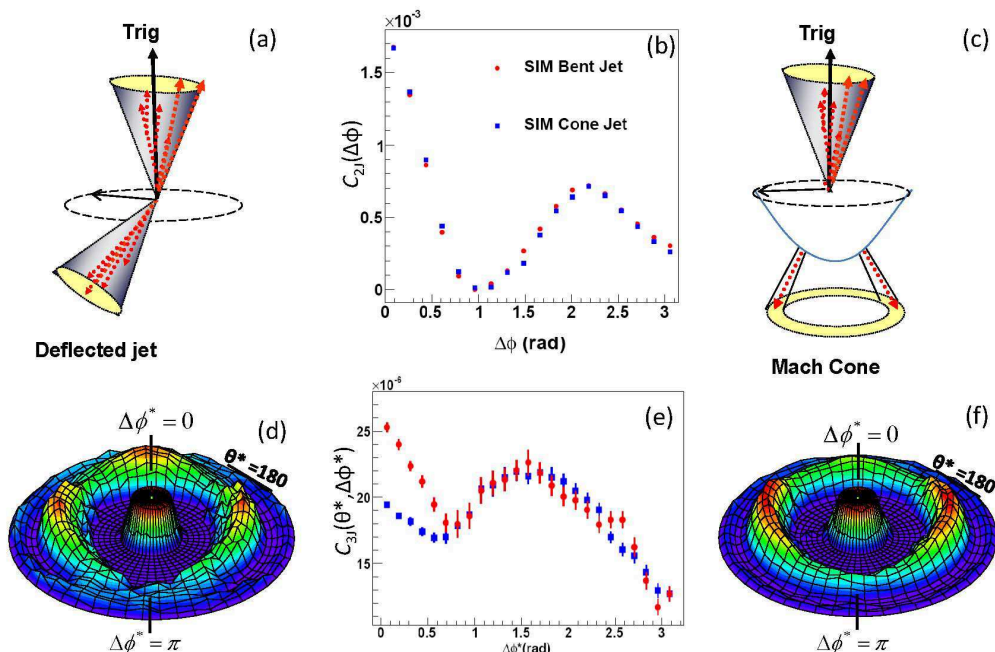


FIG. 2: (a) Schematic illustration of a bent jet topology; (b) comparison of the two-particle jet functions for bent jet and conical flow; (c) schematic illustration of conical flow topology; (d) simulated three particle correlation surface for bent jet; (f) simulated three particle correlation surface for conical flow. Panel (e) shows an azimuthal projection of both surfaces for $\theta^* \sim 120^\circ$ i.e along the ridge (see text).

side high p_T trigger and two associated particles from an away-side Mach cone, should lead to an away-side azimuthal ridge at $\theta^* = 180^\circ - \theta_M$ with no preference for $\Delta\phi^*$. Therefore, the correlation surface in Fig. 2(f), as well as its $\Delta\phi^*$ projection in Fig. 2(e) gives an indication of the relative influence of the PHENIX detector acceptance (especially in the vicinity of ϕ^* angles close to 180°) and the anomalous triplet correlations discussed above.

A. Suppression of harmonic correlations

The correlation functions shown in Fig. 2 were obtained from simulated events with hits recorded in the PHENIX acceptance from three di-jet-like particles, one trigger (high p_T) and two associated (lower p_T) particles; the underlying event particles were made isotropic. It is well known however, that there are strong harmonic correlations between the various particles and the reaction plane that follow Eq. 6. Therefore, the underlying event is not actually isotropic. Detailed systematic measurements have been made of the Fourier coefficients $v_{2,4}$ with a significantly reduced influence from jet-like correlations [14, 44]; thus, it is straightforward to incorporate these harmonic correlations into the event simulations.

A three particle correlation surface which results from the combined influence of jet-like and flow correlations is shown in Fig. 3(a). It shows that the combined correlations make it more difficult to visualize the detailed

effects of the di-jet-like emissions in the raw correlation function. This is akin to the actual experimental situation. Therefore, we wish to remove the harmonic correlation effects from the three-particle correlation surfaces. To this end we follow a procedure similar to that described in reference [42] using the ZYAM assumption i.e. we assume that the jet correlation function has zero yield at its minimum.

The three-particle correlation function which results from a combination of flow and jet-like sources can be given as

$$C_3(\theta^*, \Delta\phi^*) = a_0 [C_H(\theta^*, \Delta\phi^*) + C_J(\theta^*, \Delta\phi^*)]. \quad (8)$$

The harmonic flow correlation $C_H(\theta^*, \Delta\phi^*)$ is obtained from a flow only simulation where particles are emitted according to the measured pattern with respect to the reaction plane. The jet correlation is then given by

$$C_J(\theta^*, \Delta\phi^*) = \frac{C_3(\theta^*, \Delta\phi^*) - a_0 C_H(\theta^*, \Delta\phi^*)}{a_0}. \quad (9)$$

Applying the ZYAM condition one obtains

$$a_0 C_H(\theta_{min}^*, \Delta\phi_{min}^*) = C_3(\theta_{min}^*, \Delta\phi_{min}^*) \quad (10)$$

which can be solved to obtain a_0 .

Tests for flow removal for the case of three-particle correlation functions are shown in Fig. 3. Fig. 3(a) shows the correlation surface obtained from a simulation that

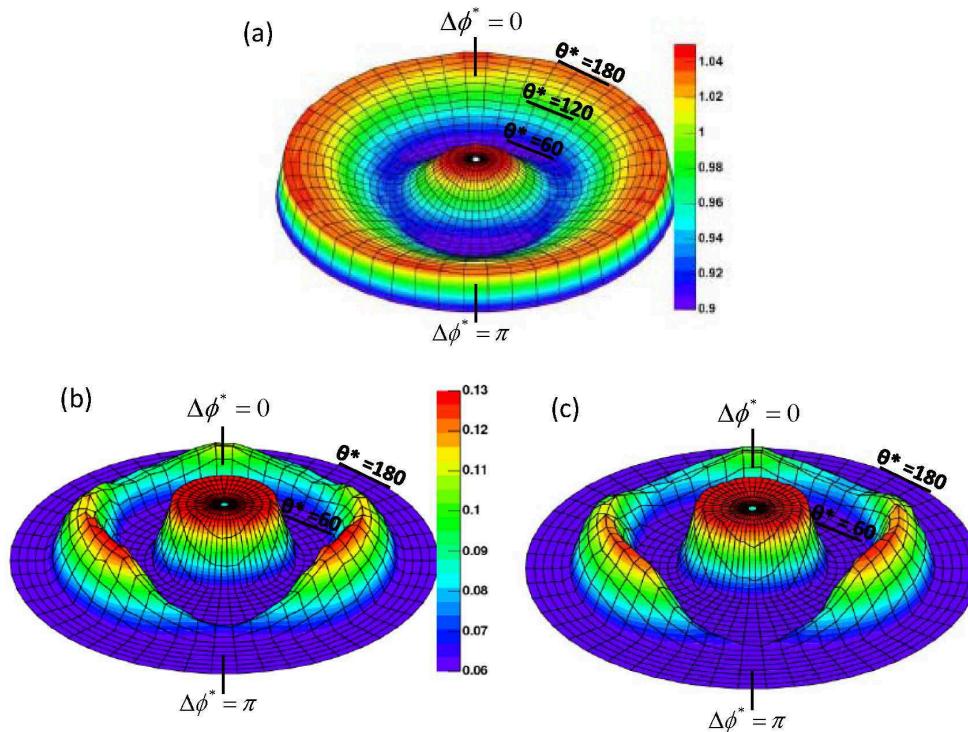


FIG. 3: (a) Simulated three particle correlation surfaces; the simulation included both flow and jet-like correlations. (b) Same as (a) but after flow subtraction. (c) Input jet-like correlations only. Note the similarity between (b) and (c).

includes both di-jet and harmonic correlations. Fig. 3(b) shows the jet function that results after removal of the harmonic correlation by the ZYAM-driven subtraction. This is to be compared to the input jet-like correlation function generated with no harmonic correlations, shown in Fig. 3(c). The similarity between Figs. 3(b) and (c) clearly show that the ZYAM procedure is able to successfully recover the essential characteristics of the input di-jet-like function.

B. Removal of (2+1) correlations

The three particle correlation function $C_J(\theta^*, \Delta\phi^*)$, obtained after removal of flow effects, still contain contributions from false triplets or (2+1)-correlations. They are of two types: (i) False “hard-soft” (hs) triplets in which the high p_T trigger and one associated low p_T particle come from the di-jet, but the second low p_T associated particle is from the underlying event. (ii) False “soft-soft” (ss) triplets in which the two low p_T associated particles belong to the same di-jet but the high p_T trigger is from the underlying event. An estimate of such correlations can be made and removed as follows. First, a (2+1)-correlation function

$$C_{(2+1)}^{(hs+ss)}(\theta^*, \Delta\phi^*) = \frac{N_{S(2+1)}(\theta^*, \Delta\phi^*)}{N_M(\theta^*, \Delta\phi^*)}, \quad (11)$$

is constructed from event pairs. Here, the distribution for fake-triplets $N_{S(2+1)}(\theta^*, \Delta\phi^*)$ is obtained by taking two particles from one event (hs or ss) and a third from another event. The hs and ss triplets are sampled in the ratio of observed ss and hs two-particle correlation strengths. As before, the mixed-events distribution $N_M(\theta^*, \Delta\phi^*)$ is obtained by taking each member of a particle triplet from a different event. This correlation function estimates both the ss and hs components of the (2+1)-contribution. Second, the flow contribution to $C_{(2+1)}^{(hs+ss)}(\theta^*, \Delta\phi^*)$ was subtracted via the procedure outlined earlier, to obtain the (2+1)-jet-like contribution $C_{J(2+1)}(\theta^*, \Delta\phi^*)$. The fully corrected triplet correlation function $C_{3J}(\theta^*, \Delta\phi^*)$ was obtained via flow and (2+1)-subtraction;

$$C_{3J}(\theta^*, \Delta\phi^*) = C_3(\theta^*, \Delta\phi^*) - H(\theta^*, \Delta\phi^*) - C_{J(2+1)}(\theta^*, \Delta\phi^*). \quad (12)$$

We have made extensive tests of this analysis procedure via detailed simulations and have confirmed its utility in suppressing both flow and (2+1)-correlations. Fig. 4(a) shows a representative comparison of the $\Delta\phi^*$ projections [along the ridge] for an input (filled circles) and a recovered (filled squares) three-particle correlation function. The recovered correlation function is obtained after removing the effects of flow and (2+1)-contributions. The comparison clearly speaks to the ef-

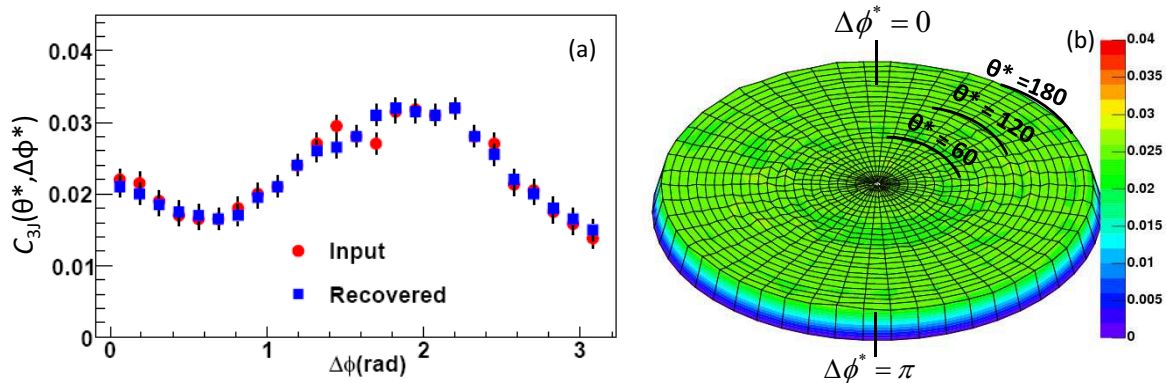


FIG. 4: (a) Comparison of the ϕ^* projections for $\theta^* \sim 120^\circ$ for simulated input and output correlation functions. The output correlation function is obtained after harmonic and (2+1) subtraction (see text); (b) correlation surface obtained from a simulation in which only (2+1)-correlations are introduced i.e no genuine three particle correlations are introduced. A small offset is added for clarity.

ficacy of the technique. A further confirmation of the efficacy of our procedure can be illustrated via the correlation surfaces obtained from simulations which include only (2+1)-correlations. One such example is given in Fig. 4(b); it shows the expected “flat” and featureless surface that is to be expected from the successful removal of (2+1)-contributions.

IV. SUMMARY

Detailed experimental probes of the hot and dense medium created in ultra-relativistic heavy ion collisions, are currently being explored via measurements of multi-hadron correlations at RHIC. These correlations contain contributions from both harmonic flow and jet-like emissions which must be disentangled, as well as topological features important to the study of the mechanism for modification of the away-side jet. A method is presented

for the analysis of such data to retrieve strongly modified jet-like topologies via three particle correlation functions. In particular, we have shown that a distinction between conical flow and a deflected (or bent) jet can be obtained in our analysis framework. Intuitively, one knows that a normal or back-to-back jet would generate a peak for the near-side jet centered at $\theta^* = 0^\circ$ and an azimuthal ridge at $\theta^* = 180^\circ$. Further, it is expected that a bent jet would lead to an away-side azimuthal ridge shifted to a θ^* angle less than 180° , but would cluster the associated away-side jet-like particles near to $\Delta\phi^* = 0^\circ$. By contrast, a Mach cone should lead to an away-side azimuthal ridge also shifted to a θ^* angle less than 180° , but without preference for any $\Delta\phi^*$ value. For the most part, these are the patterns shown by the simulations, albeit with some distortions due to the limited η acceptance of the detector and the detection of anomalous triplets. However, these distortions do not blur the topological distinction between an away-side bent jet and conical flow.

-
- [1] J. Adams et al., Nucl. Phys. **A757**, 102 (2005).
[2] K. Adcox et al., Nucl. Phys. **A757**, 184 (2005).
[3] I. Arsene et al., Nucl. Phys. **A757**, 1 (2005).
[4] B. B. Back et al., Nucl. Phys. **A757**, 28 (2005).
[5] K. Adcox et al., Phys. Rev. Lett. **89**, 212301 (2002).
[6] S. A. Voloshin, Nucl. Phys. **A715**, 379 (2003).
[7] J. Adams et al., Phys. Rev. Lett. **92**, 062301 (2004).
[8] S. S. Adler et al., Phys. Rev. Lett. **91**, 182301 (2003).
[9] J. Adams et al. (STAR), Phys. Rev. **C72**, 014904 (2005).
[10] B. Alver et al., Phys. Rev. Lett. **98**, 242302 (2007).
[11] S. S. Adler et al., Phys. Rev. Lett. **94**, 232302 (2005).
[12] S. Afanasiev et al. (PHENIX), Phys. Rev. Lett. **99**, 052301 (2007).
[13] S. Afanasiev et al. (PHENIX), Phys. Rev. **C80**, 024909 (2009).
[14] R. A. Lacey, A. Taranenko, and R. Wei (2009), 0905.4368.
[15] E. V. Shuryak, Nucl. Phys. **A750**, 64 (2005), hep-ph/0405066.
[16] R. A. Lacey and A. Taranenko, PoS **CFRNC2006**, 021 (2006).
[17] R. A. Lacey et al., Phys. Rev. Lett. **98**, 092301 (2007).
[18] H.-J. Drescher, A. Dumitru, C. Gombeaud, and J.-Y. Ollitrault, Phys. Rev. **C76**, 024905 (2007).
[19] Z. Xu, C. Greiner, and H. Stocker, Phys. Rev. Lett. **101**, 082302 (2008).
[20] H. Song and U. W. Heinz, Phys. Rev. **C78**, 024902 (2008), 0805.1756.

- [21] V. Greco, M. Colonna, M. Di Toro, and G. Ferini (2008), 0811.3170.
- [22] A. K. Chaudhuri (2009), 0909.0376.
- [23] R. Baier et al., Nucl. Phys. **B483**, 291 (1997).
- [24] M. Gyulassy et al. (2003), nucl-th/0302077.
- [25] A. Kovner and U. A. Wiedemann (2003), hep-ph/0304151.
- [26] S. S. Adler et al., Phys. Rev. Lett. **97**, 052301 (2006).
- [27] A. Adare et al. (PHENIX), Phys. Rev. **C77**, 011901 (2008), 0705.3238.
- [28] J. Adams et al. (STAR), Phys. Rev. Lett. **95**, 152301 (2005), nucl-ex/0501016.
- [29] A. Adare et al. (PHENIX), Phys. Rev. Lett. **98**, 232302 (2007), nucl-ex/0611019.
- [30] N. N. Ajitanand (PHENIX), Nucl. Phys. **A783**, 519 (2007), nucl-ex/0609038.
- [31] B. I. Abelev et al. (STAR), Phys. Rev. Lett. **102**, 052302 (2009), 0805.0622.
- [32] S. S. Adler et al. (PHENIX), Phys. Rev. **C73**, 054903 (2006), nucl-ex/0510021.
- [33] V. Koch, A. Majumder, and X.-N. Wang, Phys. Rev. Lett. **96**, 172302 (2006), nucl-th/0507063.
- [34] H. Stocker, Nucl. Phys. **A750**, 121 (2005), hep-ph/0509036.
- [35] J. Casalderrey-Solana, E. V. Shuryak, and D. Teaney, J. Phys. Conf. Ser. **27**, 22 (2005), hep-ph/0411315.
- [36] T. Renk and J. Ruppert, Phys. Rev. **C73**, 011901 (2006), hep-ph/0509036.
- [37] B. Betz, M. Gyulassy, D. H. Rischke, H. Stocker, and G. Torrieri, J. Phys. **G35**, 104106 (2008), 0804.4408.
- [38] R. B. Neufeld, B. Muller, and J. Ruppert, Phys. Rev. **C78**, 041901 (2008), 0802.2254.
- [39] P. M. Chesler and L. G. Yaffe, Phys. Rev. Lett. **99**, 152001 (2007), 0706.0368.
- [40] N. Armesto, C. A. Salgado, and U. A. Wiedemann, Phys. Rev. Lett. **93**, 242301 (2004), hep-ph/0405301.
- [41] C. B. Chiu and R. C. Hwa, Phys. Rev. **C74**, 064909 (2006), nucl-th/0609038.
- [42] N. N. Ajitanand et al., Phys. Rev. **C72**, 011902 (2005), nucl-ex/0501025.
- [43] K. Adcox et al., Nucl. Instrum. Meth. **A499**, 469 (2003).
- [44] pp098 (2009), nucl-ex/xxx.yyy.